Revista Mexicana de Astronomía y Astrofísica, **42**, 41–46 (2006)

PRESERVATION OF CUSPY PROFILES IN DISK GALAXY MERGERS

H. Aceves and H. Velázquez

Instituto de Astronomía
Universidad Nacional Autónoma de México, Ensenada, B. C., México

Received 2005 May 27; accepted 2005 November 7

RESUMEN

Se efectuaron tres simulaciones auto-consistentes de N-cuerpos de fusiones entre galaxias, con un perfil pronunciado de materia oscura, para estudiar si la pendiente interna del perfil de densidad oscura se preserva en los remanentes. En estas simulaciones los progenitores incluyen un disco estelar y un espín intrínsico en el halo a diferencia de estudios similares. La razón de masas de las galaxias progenitoras es de alrededor de 1:1, 1:3 y 1:10. Encontramos que el perfil de densidad inicial pronunciado de los halos oscuros se preserva en los remanentes para los casos considerados aquí.

ABSTRACT

We carried out three self-consistent N-body simulations of galaxy mergers, with a cuspy dark matter profile, in order to study if the inner dark density slope is preserved in the remnants. In these simulations the progenitors include both a stellar disk and an intrinsic angular momentum for the halos, unlike previous similar studies. The mass-ratios of progenitor galaxies are about 1:1, 1:3, and 1:10. We find that the initial cuspy density profile of the dark halos is preserved in the remnants for the cases considered here.

Key Words: **GALAXIES: INTERACTIONS — GALAXIES: KINEMATICS AND DYNAMICS — METHODS: *N*-BODY SIMULATIONS.**

1. INTRODUCTION

High-resolution simulations of hierarchical structure formation within the ΛCDM cosmogony show that the inner regions of the halos follow a power-law cusp, $\rho \propto r^{-\gamma}$, with $1 \leq \gamma \leq 1.5$ while in their outer parts the profiles go as $\rho \propto r^{-3}$ over a wide range of mass-scales (e.g., Navarro, Frenk, & White 1997, hereafter NFW; Moore et al. 1999, hereafter M99; Fukushige, Kawai, & Makino 2004; Navarro et al. 2004).

The physical origin of this profile is still unclear and it is the subject of an intense investigation. Nevertheless, there is a certain agreement in the sense that such a density profile is linked to the accretion and merging history of the dark matter substructures (e.g., Syer & White 1998, Dekel; Devor & Hetzroni 2003; Williams, Babul, & Dalcanton 2004).

Several authors have studied the shape and survival of the density profile inner slope in collisionless mergers (e.g., White 1978, Fulton, & Barnes 2001; Boylan-Kolchin & Ma 2004). In the early study of White (1978) it was found that mergers of cored galaxies were more concentrated than their progenitors. Fulton & Barnes (2001) found in their N-body experiments that steep cusps are preserved during mergers of equal-mass progenitors. Boylan-Kolchin & Ma (2004, hereafter BKM) concluded that if two galaxies merge having each one a core-type profile the resulting remnant will be core-type, and if one progenitor has a cuspy profile then the remnant will also be cuspy. This result is in agreement with other simulations (Moore et al. 2004).

This type of studies find justification in that, although in a collisionless simulation the phase-space density must be conserved, due to Liouville's theorem, there is no a priori reason to expect that both configuration and momentum distributions are to be conserved independently (BKM).

A common feature of previous related works is that they consider gravitational systems with only

a spherical or dark matter component, and they do not consider the effect, for example, that a disk or an intrinsic halo spin might have on the preservation of cusps during a merger process. This needs to be addressed since there are several studies that indicate that angular momentum may play a key role at the time of formation of the halo, as well as on the shape of the density profile within the inner regions, by preventing that dark matter particles reach the inner regions, resulting in a shallower central profile (e.g., White & Zaritsky 1992; Hiotelis 2002; Ascasibar et al. 2004). Furthermore, cosmological simulations lead to dark halos having an intrinsic angular momentum (Barnes & Efstathiou 1987; Lemson & Kauffmann 1999).

In this work we study three numerical N-body simulations of progenitor self-consistent disk galaxies with mass-ratios of about 1:1, 1:3, and 1:10, following parabolic encounters. The present work expands on earlier similar studies mainly in that the progenitors have a disk component and their halos have an intrinsic angular momentum. This would allows us to test, using more realistic initial conditions, if the cuspy nature of the progenitor galaxies is preserved in mergers at the resolution provided by our N-body simulations.

The rest of this paper has been organized as follows. In § 2 we describe the theoretical method used to construct the galaxy models, the properties of their dark halos, especially the behavior of the inner logarithmic derivative and the initial conditions for the encounters. In § 3 we present our results, and in § 4 we summarize our main results.

2. MERGER MODEL

2.1. *Disk Galaxies*

Our galaxy models consist of a spherical halo and a stellar disk; no bulge component is included. The disk is represented by an exponential profile in the radial direction and by an isothermal sheet in the vertical one (Hernquist 1993):

$$\rho_{\rm d}(R,z) = \frac{M_{\rm d}}{4\pi R_{\rm d}^2 z_d} \exp(-R/R_{\rm d}) \,{\rm sech}^2(z/z_d)\ , \quad (1)$$

where $R_{\rm d}$ and $z_{\rm d}$ are the radial and vertical scale-lengths of the disk, respectively.

For the dark halo, a spherical model is adopted by assuming a NFW-profile with an exponential cutoff:

$$\rho_{\rm h}(r) = \frac{M_{\rm h}\,\alpha_{\rm h}}{4\pi r (r+r_{\rm s})^2}\ \exp\left[-\left(\frac{r}{r_{200}}+q\right)^2\right]\ , \quad (2)$$

where $r_{\rm s}$ and r_{200} are the the scale and "virial" radii, respectively, $c = q^{-1} = r_{200}/r_{\rm s}$ and $M_{\rm h}$ are the concentration and the mass of the halo. The r_{200} is defined in cosmological simulations as the radius where the mean interior density is 200 times the critical density. In general, r_{200} is not exactly the virial radius (§2.4), but is a good approximation to it and serves to characterize the halo (NFW, Cole & Lacey 1996).[1] Here, $\alpha_{\rm h}$ is a normalization constant given by

$$\alpha_{\rm h} = \frac{\exp(q^2)}{\sqrt{\pi} q \exp(q^2){\rm Erfc}(q) + \frac{1}{2}\exp(q^2){\rm E}_1(q^2) - 1}\ ,$$

where ${\rm Erfc}(x)$ is the complementary error function and ${\rm E}_1(x)$ the exponential integral.

The radial scale length of the disk is obtained accordingly to the Mo, Mao, & White (1998) framework of disk galaxy formation. To determine this quantity five parameters are required, namely: the circular velocity $V_{\rm c}$ at r_{200}, the dimensionless spin parameter λ, the concentration c of the dark halo, the fraction of disk to halo mass $m_{\rm d}$, and the fraction of angular momentum in the disk to that in the halo $j_{\rm d}$. We followed the method described by Shen, Mo, & Shu (2002) to obtain these parameters. A ΛCDM cosmology is adopted with a mass density of $\Omega_0 = 0.3$ and with a contribution due to the cosmological constant of $\Omega_\Lambda = 0.7$.

The selected galaxy disks satisfy a stability criterion $\varepsilon_{\rm m} \geq 0.9$; where $\varepsilon_{\rm m}{=}V_{\rm m}(GM_{\rm d}/R_{\rm d})^{-1/2}$, $V_{\rm m}$ being the maximum rotation velocity (Efsthatiou, Lake, & Negroponte 1982; Syer, Mao, & Mo 1997). Mass-ratios of about 1:1, 1:3, and 1:10 were chosen to study the properties of the merger remnants. Finally, the velocities of particles were set up through Jeans equations following the method prescribed by Hernquist (1993).

In Table 1 we list the parameters defining our galaxy models; below the merger simulation label ($S1$, $S2$, and $S3$) the mass ratio of the secondary to the primary galaxy has been indicated. The number of particles in the halo $N_{\rm h}$ and in the disk $N_{\rm d}$ is also listed.

2.2. *Encounter Parameters*

Only parabolic encounters are considered for the binary mergers. The relative initial separation between both galaxy centers is taken to be

$$R_{\rm s} = 1.25\,(r_{200,1} + r_{200,2})\,, \quad (3)$$

[1] The virial radii of the disk numerical models in § 2.4 turn out to be ≈ 20% smaller than the r_{200} in Table 1.

TABLE 1

INITIAL GALAXIES

Merger	Halo Properties						Disc Properties			
M_s/M_p	M_h $[M_\odot]$	r_{200} [kpc]	λ	j	c	N_h	M_d $[M_\odot]$	R_d [kpc]	z_d [kpc]	N_d
$S1$	4.74×10^{11}	110.3	0.112	0.106	11.39	240000	4.16×10^{10}	6.6	1.29	60000
0.14	6.99×10^{10}	58.3	0.071	0.035	9.94	165992	2.88×10^{9}	1.6	0.19	48689
$S2$	4.02×10^{11}	104.3	0.063	0.041	7.63	57126	2.11×10^{10}	2.4	0.39	12000
0.32	1.25×10^{12}	152.3	0.056	0.068	3.84	177571	7.78×10^{10}	5.7	0.47	44267
$S3$	8.11×10^{10}	61.2	0.099	0.142	10.87	150000	7.22×10^{9}	4.6	0.73	30000
0.98	8.33×10^{10}	61.8	0.122	0.095	10.01	154050	7.15×10^{9}	3.9	0.56	29686

where $r_{200,1}$ and $r_{200,2}$ are, respectively, their r_{200} "virial" radii.

Orbital angular momentum is introduced in the simulations by randomly choosing a pericenter for each encounter, assuming that galaxies are point particles in a Keplerian orbit. Pericentric radii in the range $R_p = \{5-20\}$ kpc were adopted. These values for the orbital parameters are consistent with those found in cosmological N-body simulations and tend to favor mergers (Navarro, Frenk, & White 1995). The relative orientation of the spin vector of the galaxies relative to the orbital plane of the encounter is chosen randomly.

2.3. *Numerical Tools*

These N-body simulations were performed using a parallel version of GADGET, a tree base code with individual timesteps (Springel, Yoshida, & White 2001). The runs were made in a Pentium based cluster of 32 processors (Velázquez & Aguilar 2002). Softening parameters $\epsilon_d = 35\,\mathrm{pc}$ and $\epsilon_h = 350\,\mathrm{pc}$ for disk and halo particles, respectively, were used. Since GADGET uses a spline kernel for the softening, the gravitational interaction between two particles is fully Newtonian for separations larger than twice the softening parameters (Power et al. 2003).

The typical time of arrival of the galaxies to the first passage through pericenter is about 1 Gyr. We follow each encounter for a total time of about 8 Gyr. At this time the remnants had reached a stable value close to virial equilibrium. Energy conservation was better than 0.25% in all our simulations.

2.4. *Resolution Criteria and Stability of Initial Dark Halo Profiles*

The two-body relaxation time-scale imposes an inner 'convergence' radius r_c over which the stellar system can be adequately described by a collisionless distribution function (e.g., Power et al. 2003; Hayashi et al. 2004; Diemand et al. 2004; Binney 2004).

Here, we take r_c as the radius where its local two-body relaxation time-scale t_r is equal to the period T_v of a circular orbit at the virial radius; i.e., r_c satisfies

$$\frac{t_r(r)}{T_v} = \frac{N}{8\ln N}\frac{r}{V(r)}\frac{V_v}{r_v} = 1\,, \qquad (4)$$

where V_v is the circular velocity at the virial radius, r_v, and $N = N(r)$ the total number of particles inside a radius r. The virial radius is $r_v = GM_t/|W|$, M_t being the total mass of all bound particles and W the total potential energy.

For each initial galaxy we computed spherically averaged density profiles, $\rho(r)$, in a logarithmically spaced grid within r_c and r_v; in general, we find $r_c/r_v \approx 0.01$. To check that the dark density profile of our initial galaxy models does not change, we evolved in isolation each galaxy for about 8 Gyr, that corresponds to ≈ 25 dynamical times, $t_{dyn} = \sqrt{3\pi/16G\bar{\rho}_h}$; where $\bar{\rho}_h$ is the mean density at the half-mass radius. At this time the virial ratio fluctuates within $\lesssim 1\%$ from the ideal value of unity, and no significant change in the density profiles is observed; see Figure 1.

Results in the literature (e.g., Kazantzidis, Magorrian, & Moore 2004; Springel, Di Matteo, & Hernquist 2005) indicate that obtaining the velocities of particles using the Hernquist (1993) procedure, that assumes a Maxwellian local velocity distribution, is inadequate. In these works it is found that models evolved in isolation tend to relax rapidly to an inner density slope shallower than the initial condition. However, our models constructed using

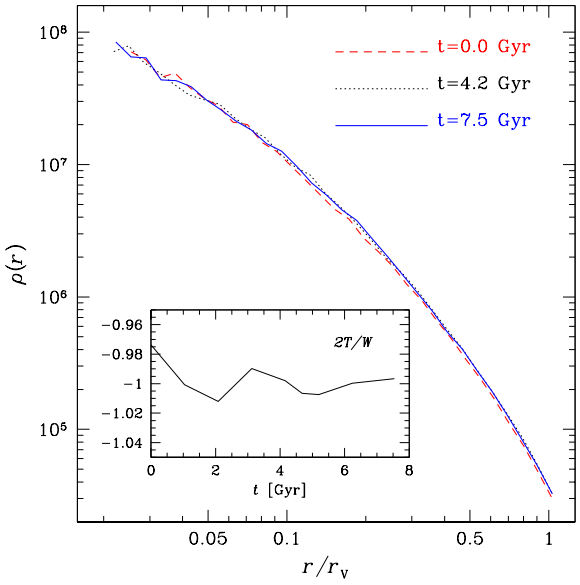

Fig. 1. Density profiles of the dark matter component at different times of a galaxy model evolved in isolation. Different lines indicate the time spent in isolation. The dynamical time is $t_{\rm dyn} \approx 0.3\,$Gyr, so the evolution is over $\approx 25 t_{\rm dyn}$. The inner profile, close to $r_{\rm c}$, remains stable showing no shallowing of the density slope. The inset indicates the evolution of the virial ratio.

Hernquist's method do not show a shallowing of the inner slope when evolved in isolation (see Fig. 1).

We fitted NFW density profiles,

$$\rho_*(r) = \frac{\rho_{\rm s}}{(r/\bar{r}_{\rm s})(1+r/\bar{r}_{\rm s})^2}\,, \qquad (5)$$

to the $\rho(r)$ of the initial numerical models; here, $\bar{r}_{\rm s}$ is the scale radius. The fitting was done by χ^2-minimization using the Levenberg-Marquardt method (Press et al. 1992). From the fitted profile we computed the logarithmic derivative $\beta(r) = {\rm d}\log\rho/{\rm d}\log r$.

To verify that our binning method does not affect the fitting of the density profiles, we computed $\rho(r)$ in bins of equal number of particles, from 100 to 1500, and the parameters of the fitted profile did not change significantly ($\lesssim 1\%$) in comparison to the logarithmically spaced grid. We consider that this provides a good degree of confidence in the results presented for our fits.

The mean RMS of the deviations, $\delta = (\rho - \rho_*)/\rho$, for the initial profiles in the complete fitting interval is 0.120, while for the inner region (up to a radius of 10% of the virial radius) a mean value, $\rm RMS_{10}$, of 0.078 is obtained. The latter value is an indication that the N-body realization follows closely a NFW profile at the inner region.

TABLE 2

INITIAL GALAXY SLOPES

Merger	N-body Model		
$M_{\rm s}/M_{\rm p}$	RMS	$\rm RMS_{10}$	$-\beta_{\rm c}$
$S1$	0.098	0.046	1.25
0.14	0.115	0.068	1.22
$S2$	0.128	0.105	1.28
0.32	0.178	0.120	1.06
$S3$	0.102	0.075	1.12
0.98	0.100	0.053	1.32

We estimated the logarithmic derivative at $r_{\rm c}$, $\beta_{\rm c}$, for each individual galaxy, and a mean value of -1.21 was found. Individual values of $\beta_{\rm c}$ and RMS, both total and inside $0.10R_{\rm v}$, are listed in Table 2. We note that the values of $\beta_{\rm c}$ differ from each other since $r_{\rm c}$ for each progenitor is different.

3. MERGER DENSITY PROFILES

In Figure 2 we show the time evolution of the dark matter density profile for merger $S2$, from $\approx 6\,$Gyr to $\approx 8\,$Gyr. As observed, the inner density profile does not change significantly from $\approx 6\,$Gyr to the end of the simulation. The evolution of the virial ratio for the whole time of the simulation is shown in the inset. The dynamical time of the remnant is $t_{\rm dyn} \approx 0.4\,$Gyr, so for $\approx 5 t_{\rm dyn}$ the profile remains unchanged and the virial ratio has settled to the equilibrium value around 1, with some numerical fluctuations less than 1%. A similar behavior in the profile and virial ratio was observed for the other two simulations considered. The analysis of the resulting profile of the remnants was done at $t \approx 8\,$Gyr.

A NFW profile was fitted to the resulting merger remnants. The fitting is done in their corresponding interval $(r_{\rm c}, r_{\rm v})$. In Table 3 we present the values for the total RMS deviation of the fit (Col. 2), the RMS inside $0.1r_{\rm v}$ (Col. 3), the scale radius $\bar{r}_{\rm s}$ in kpc (Col. 4), the concentration parameter $\bar{c} = r_{\rm v}/\bar{r}_s$ (Col. 5), and the logarithmic derivative at $r_{\rm c}$ obtained from the fitting (Col. 6).

In Figure 3 (*top*) we show the fractional residuals of the merger fittings to a NFW profile and (*bottom*) the numerical logarithmic derivatives of the data that correspond to the fitted profile (5). Though the numerical logarithmic derivatives are rather noisy, especially at the boundaries of the fitting region, they follow on average the $\beta(r)$ obtained from the

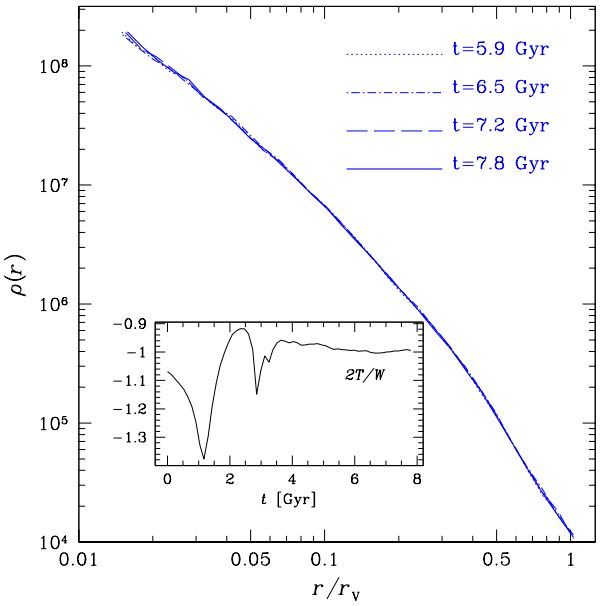

Fig. 2. Late time evolution of the density profile of the remnant of simulation $S2$, from $\approx 6\,$Gyr to $\approx 8\,$Gyr. The dynamical time of the remnant is $t_{\rm dyn} \approx 0.4\,$Gyr. The inset shows the virial ratio during the total time of the simulation.

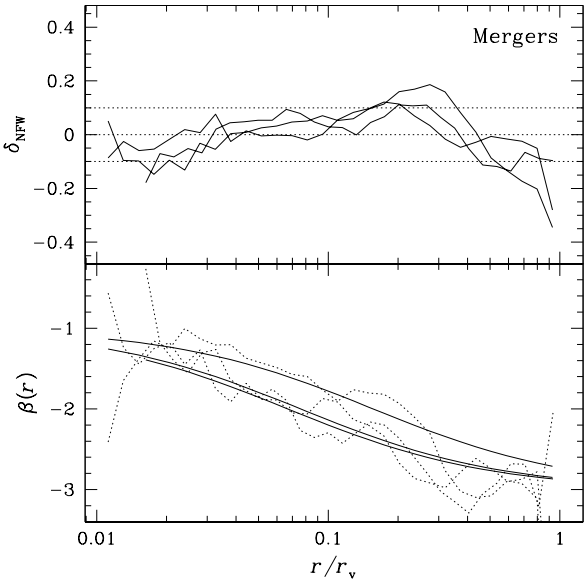

Fig. 3. (*Top*) Fractional residuals, $\delta_{\rm NFW} = (\rho - \rho_{\rm NFW})/\rho$, of the mergers' density profiles with respect a NFW profile. (*Bottom*) Numerical logarithmic derivatives (dotted lines) and the ones obtained from the fitted profile (continuous lines).

TABLE 3

REMNANTS' NFW PROFILE.

Merger	Profile Parameters				
	RMS	$\rm RMS_{10}$	$\bar{r}_{\rm s}$	$\bar{c}$	$-\beta_{\rm c}$
$S1$	0.074	0.040	5.69	13.17	1.24
$S2$	0.124	0.078	24.40	6.39	1.12
$S3$	0.082	0.081	4.42	14.96	1.37

fits. The mean RMS of the density fits for the entire interval is 0.093, while for the region from $r_{\rm c}$ up to $0.10 r_{\rm v}$ is about 0.066. On other hand, the average value of $\beta_{\rm c}$ obtained for the remnants is -1.24.

The mean $\rm RMS_{10}$ in the fits of the remnants is about the same as that found in the fit for the progenitors to the NFW profile. The values of $\beta_{\rm c}$ of the remnants (Table 3) do not necessarily need to coincide with, say, the average value of their progenitors (Table 2) since $r_{\rm c}$ is different in both cases. We consider the $\rm RMS_{10}$ of these fits to be a better indicator of the preservation of the initial cuspy profile at the inner region.

There has been some discussion (e.g., Navarro et al. 2004) on whether a profile of the form proposed

TABLE 4

REMNANTS' M99 PROFILE.

Merger	Profile Parameters				
	RMS	$\rm RMS_{10}$	$r_{\rm M}$	$\tilde{c}$	$-\beta_{\rm c}$
$S1$	0.084	0.093	10.56	7.09	1.53
$S2$	0.196	0.219	47.03	3.32	1.51
$S3$	0.077	0.099	7.98	8.29	1.56

by M99,

$$\rho(r) = \frac{\rho_{\rm M}}{(r/r_{\rm M})^{1.5}[1 + (r/r_{\rm M})^{1.5}]} \,, \qquad (6)$$

provides a better fit to the dark halos. We tested also if (6) provided a better fit to the density profiles of the remnants. In Table 4 we list the values obtained for similar quantities as those in Table 3; but with $\tilde{c} = r_{\rm v}/r_{\rm M}$. In Figure 4 we show the fractional residuals of the fits and $\beta(r)$ using (6).

We find a mean $\beta_{\rm c} = -1.53$ but with the average $\rm RMS_{10}$ to be 0.137, a value that is $\approx 100\%$ larger than that obtained with the NFW profile inside $0.1 R_{\rm v}$. We take this result as an indication that the M99 profile does not provides a good fit to our merger remnants.

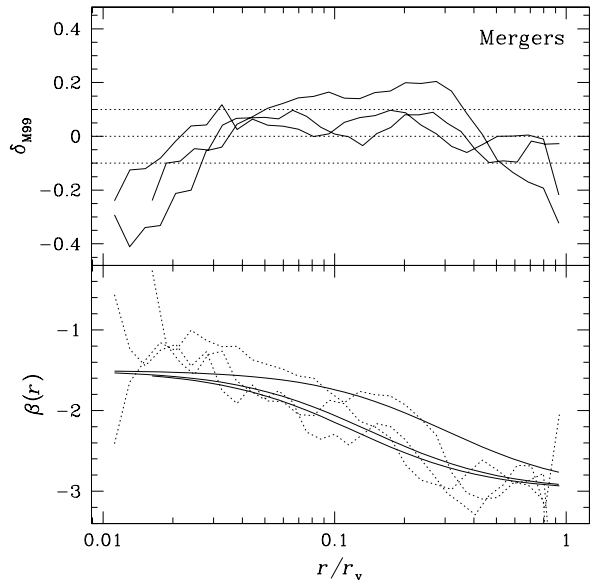

Fig. 4. (*Top*) Fractional residuals, $\delta_{M99} = (\rho - \rho_{\rm M99})/\rho$, of the mergers' density profiles with respect to a M99 profile. (*Bottom*) numerical logarithmic derivatives (dotted lines) and the ones obtained from the assumed profile (continuous lines).

4. SUMMARY

We have built up disk galaxies using the cosmologically motivated model of MMW to study the cuspiness properties of merger remnants. The progenitor galaxies have spin in their halos and mass-ratios of about 1:10, 1:3, and 1:1. This work was restricted to the study of binary mergers following parabolic encounters.

Our results indicate that angular momentum, both intrinsic and orbital, does not change the behavior of the density profile inside the inner regions of a merger remnant.

However, taking into account that few simulations were done, we can not completely rule out the effect of the initial angular momentum of the system on the inner density profile of the remnants. A wider set of simulations is required to check the result found here.

We thank CONACyT, México, for financial support through Project 37506-E. An anonymous referee is thanked for providing important comments that helped to improve the presentation of this work.

REFERENCES

Ascasibar, Y., Yepes, G., & Gottlöber, S., & Müller, V. 2004, MNRAS, 352, 1109
Barnes, J., & Efstathiou, G. 1987, ApJ, 319, 575
Binney, J. 2004, MNRAS, 350, 939
Boylan-Kolchin, M., & Ma, C. 2004, MNRAS, 349, 1117 (BKM)
Cole, S., & Lacey, C. 1996, MNRAS, 281, 716
Dekel, A., Devor, J., & Hetzroni, G. 2003, 341, 326
Diemand, J., Moore, B., Stadel, J., & Kazantzidis, S. 2004, MNRAS, 348, 977
Efstathiou, G., Lake, G., & Negroponte, J. 1982, MNRAS, 199, 1069
Fukushige, T., Kawai, A., & Makino, J. 2004, ApJ, 606, 625
Fulton, E., & Barnes, J. E. 2001, Ap&SS, 276, 851
Hayashi, E., Navarro, J. F., Power, C., et al. 2004, MNRAS, 355, 794
Hernquist, L. 1993, ApJS, 86, 389
Hiotelis, N. 2002, A&A, 382, 84
Kazantzidis, S., Magorrian, J., & Moore, B. 2004, ApJ, 601, 37
Lemson, G., & Kauffmann, G. 1999, MNRAS, 302, 111
Mo, H. J., Mao, S., & White, S. D. M. 1998, MNRAS, 295, 319 (MMW)
Moore, B., Kazantzidis, S., Diemand, J., & Stadel, J. 2004, MNRAS, 354, 522
Moore, B., Quinn, T., Governato, F., Stadel, J., & Lake, G. 1999, MNRAS, 310, 1147 (M99)
Navarro, J. F., Frenk, C. S., & White, S. D. M. 1995, MNRAS, 275, 56
_____. 1997, ApJ, 490, 493 (NFW)
Navarro, J. F., Hayashi, E., Power, C., et al. 2004, MNRAS, 349, 1051
Press, W. H., Teukolsy, S. A., Vetterling, W. T., & Flannery, B. P. 1992, Numerical Recipes: The Art of Scientific Computing (New York: Cambridge Univ. Press)
Power, C., Navarro, J. F., Jenkins, A., Frenk, C. S., White, S. D. M., Springel, V., Stadel, J., & Quinn, T. 2003, MNRAS, 338, 14
Shen, S., Mo, H. J., & Shu, C. 2002, MNRAS, 331, 251
Springel, V., Di Matteo, T., & Hernquist, L. 2005, MNRAS, 361, 776
Springel, V., Yoshida, N., & White, S. D. M. 2001, NewA, 6, 79
Syer, D., Mao, S., & Mo, H. J. 1997, `astro-ph/9711160`
Syer, D., & White, S. D. M. 1998, MNRAS, 293, 337
Velázquez, H., & Aguilar, L. 2003, RevMexAA, 39, 197
White, S. D. M. 1978, MNRAS, 184, 185
White, S. D. M., & Zaritsky, D. 1992, ApJ, 394, 1
Williams, L. L. R., Babul, A., & Dalcanton, J. J. 2004, ApJ, 604, 18

Héctor Aceves and Héctor Velázquez: Instituto de Astronomía, UNAM, Apdo. Postal 877, 22800 Ensenada, B. C., México (aceves@astrosen.unam.mx; hmv@astrosen.unam.mx).